UNDERSTANDING CURRENTS AND WAVES BY MEASURING ELECTRIC AND MAGNETIC FIELDS WITH SOUNDING ROCKETS

Paul M. Kintner, Jr.

School of Electrical and Computer Engineering, 302 Rhodes Hall, Cornell University, Ithaca, NY 14853 USA, Email: pmk1@cornell.edu

ABSTRACT

New technology leads to new discoveries. We have created a self-contained sounding rocket subpayload that measures electric fields and magnetic fields as accurately as satellites but on a much slower moving platform so that precise dynamics in the fields and currents can be obtained. Called COWBOYS for COrnell Wire BOom Yo-yo System, this new instrument yields data that allow us to characterize the Alfvénic region on the poleward boundary of the auroral oval during active periods. Multiple subpayloads help us resolve space-time ambiguities and validate the small perturbing magnetic fields produced by field-aligned currents. We have found regions of downward locally accelerated electrons, transversely accelerated ions, and inertial Alfvén waves embedded in a region of rapidly varying Poynting flux. Hence this region of space is likely the mass source for heavy ions in the magnetosphere. Understanding how the Alfvén waves energize ions is a central goal of this research.

1. INTRODUCTION

The northern lights exist in two forms. One form is quasi-static in which the ionosphere and magnetosphere are in equilibrium. The other form is dynamic in which electric fields and currents are changing rapidly and the ionosphere and magnetosphere are not in equilibrium. Equilibrium is determined by whether information is communicated between the ionosphere and magnetosphere on time scales that are fast compared to the time scales by which the ionosphere and magnetosphere are changing. If the time scales for exchanging information are not faster than the dynamic time scales, there is no equilibrium. Information is exchanged between the ionosphere and magnetosphere via Alfvén waves. To be in equilibrium, Alfvén waves must transit several times back and forth between the ionosphere and magnetosphere with time scales of seconds to tens of seconds. The auroras are the most attractive and most physically significant when they are changing the most rapidly. Hence Alfvén waves play an important role in magnetosphere-ionosphere coupling.

The importance of Alfvén waves in space plasmas has long been known, but perhaps the first detailed experimental investigation of Alfvén waves in magnetosphere-ionosphere coupling was with sounding rockets [1]. Later, satellite experiments confirmed the existence of an Alfvén region on the poleward boarder of the auroral oval during periods of auroral activity [2] in which large amplitude, fluctuating electric and magnetic fields were present. In the Alfvén region, electrons of a few hundred eV to a few keV were found to accelerate downward in field-aligned bursts that look dispersive in energy-time plots where the dispersion arises from fast, localized acceleration over a broad energy range, followed by faster transit times for more energetic electrons. Also found in the Alfvén region are transversely accelerated heavy ions (O^+) that start at about 0.2 eV and are energized to a few hundred eV.

Given the importance of the Alfvén region, we have developed an instrument, COWBOYS, for investigating the electric and magnetic fields that characterize Alfvén waves. In this brief article, we describe the COWBOYS instrument and illustrate measurements made with the instrument on the SIERRA (Sounding of the Ion Energization Region: Resolving Ambiguities) sounding rocket. Since the original flight of COWBOYS made on SIERRA, six more COWBOYS instruments have been included in four sounding rocket experiments.

2. THE COWBOYS INSTRUMENT

The goal of the COWBOYS instrument is to accurately and instantaneously measure a 2-D electric field and a 3-D magnetic field while determining its position to within a few meters and maintaining its time synchronization to better than 1 μsec. An additional goal is to utilize inexpensive and easily accessible hardware. We accomplished these goals by creating a system that used wire booms, a magneto-viscous damper, and a Cornell-designed GPS receiver on a dedicated subpayload. Figs. 1 and 2 show two different views of the COWBOYS instrument and subpayload.

In Fig. 1, two COWBOYS instruments and subpayloads are present. The electric field instrument

Proc. '19th ESA Symposium on European Rocket and Balloon Programmes and Related Research, Bad Reichenhall, Germany, 7–11 June 2009 (ESA SP-671, September 2009)

is the upper half of the payload while the lower half of the payload contains the telemetry transmitter and antenna built by NASA/WFF. In addition, the lower half contains a Cornell magnetometer instrument.

The electric field instrument visible in Fig. 1 is the spiral winding and the four spheres mounted on top of the aluminum can. Inside the aluminum can is a

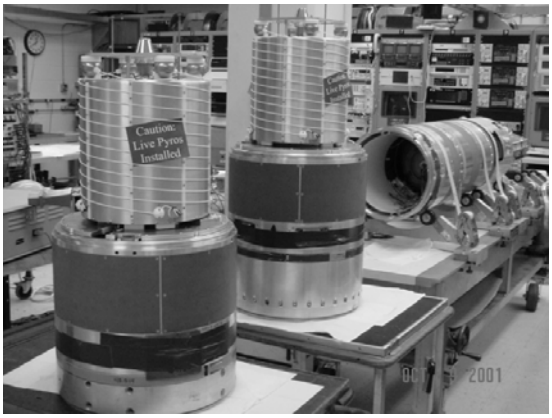

Figure 1. The COWBOYS instruments and sub-payloads for the SIERRA experiment.

magneto-viscous brake. The aluminum can differentially rotates with respect to the telemetry section while the viscosity of the brake can be controlled electronically. At deployment, a capture cage is ejected, deploying all of the four spheres simultaneously. As the wires unwind, the differential rotation of the top and bottom of the payload is monitored and the differential rotation is controlled by electronically controlling the viscosity of the magneto-viscous brake. In this way, all excess energy is removed just as the wires become radial. To make the system stable, it is designed so that the root of the wire booms passes through the center of mass. Also, the entire subpayload is dynamically balanced.

To make this system inexpensive, we use a magneto-viscous brake originally designed for stationary bicycles. The aluminum can is machined from a turkey frying pot, and the conducting spheres used to make electrical contact with the ionospheric plasma are float valves from high-end commodes. Typically, the electrical signals are divided into two bands, DC-250 Hz and 20 Hz-16 kHz, with a resolution of 100 μV/m.

The magnetometer is mounted in the bottom of the subpayload as shown in Fig. 2. The magnetometer is a 3-axis fluxgate Billingsley Magnetics TFM100-LN-CL, ±60,000 nT, with a frequency response of 0-300 Hz (-3 dB). The noise level is ≤14 picoTesla RMS/sqrt (Hz) and a 16-bit ADC yields a resolution of 2 nT. Because power consumption is stable, variable-noise magnetic fields are not present. The magnetometer is initially calibrated on the ground and then calibrated in flight using an entire-flight optimization algorithm, taking into account alignment errors and payload-bias magnetic fields.

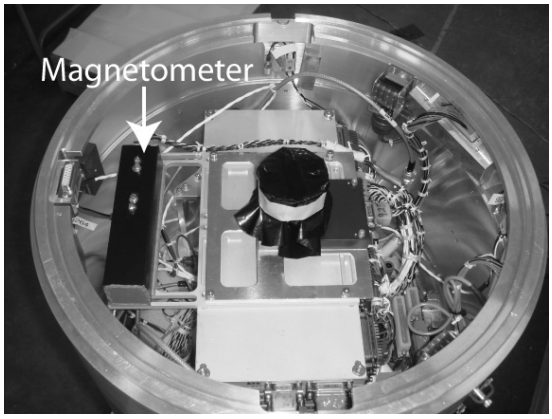

Figure 2. Bottom view of the SIERRA subpayload showing the magnetometer.

The telemetry system on the subpayload is synchronized with the Cornell University COUGAR receiver [3] built around a Zarlink-Plessey chip set. The GPS antenna is incorporated into the wrap-around telemetry antenna visible in Fig. 1. Relative positioning of the two payloads during flight was achieved with an accuracy of about 5 m.

3. THE SIERRA SOUNDING ROCKET EXPERIMENT

The SIERRA sounding rocket was launched from the Poker Flat Research Range on January 14, 2002 at 0823:05 UT into a westward-traveling surge characterized by a modest magnetic bay of -100 nT. The payload reached an apogee of 735 km near 492 s flight time. The payload was composed of two COWBOYS subpayloads and a main payload with particle and field instrumentation as well as electric and magnetic field instrumentation. The main payload contained a conventional electric field sensor for comparison with the COWBOYS wire boom and sphere sensors.

During the first half of the flight, SIERRA passed through several stable arcs, as evidenced by inverted-V electron precipitation measured on the main payload, and then an Alfvénic region from roughly 520-700 s flight time, followed by entry into the polar cap. The Alfvénic region contained dispersed electron bursts, transversely accelerated ions, and fluctuating electric and magnetic fields, which are described in the next section.

Fig. 2 shows the orientation of the main payload and subpayloads during flight along the velocity vector with respect to geographic coordinates and ionospheric coordinates. Both geographic and geomagnetic coordinates are also sketched.

The two subpayloads in Fig. 3 are labeled forward and aft, referring to their location with respect to the main payload at launch. After launch and after exiting the atmosphere, an attitude control system (ACS) orients the bottom of the payload to point along the trajectory and ejects the aft subpayload. The aft subpayload then

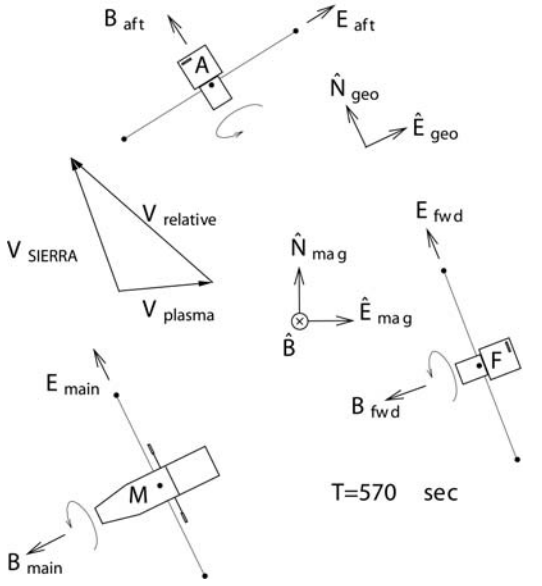

Figure 3. Configuration of the SIERRA main payload and subpayloads showing the electric field boom orientations and magnetic field instrument orientation.

appears to be in "propeller mode". The front of the payload is then oriented in the eastward direction and the forward subpayload is ejected. The forward subpayload and main payload appear to be in "wagon wheel" mode. The overall configuration would be a right angle triangle with the main payload at the vertex of the right angle, except for the fact that the main payload recoils at ejection. Fortunately, the GPS receivers provide accurate positioning, so the dynamics are well known.

The ejection velocities of both COWBOYS subpayloads were about 1.6 m/s, leading to an overall separation near apogee of 500 m between the aft and main payloads and 650 m between the forward and main payloads. The larger separation between the forward and main payloads arose because of the larger recoil velocity of the main payload during ejection.

An important feature of the payload and subpayload orientations is that the main and forward payloads are measuring the electric field in parallel planes defined by the magnetic field and geographic north. Also, the spin axis components of their magnetometers are parallel. On the other hand, the aft subpayload is measuring the electric field in the plane defined by the magnetic field and geographic east while the spin axis component of the aft subpayload is perpendicular to the spin axis component of the other two magnetometers.

4. RESULTS FROM THE SIERRA EXPERIMENT

The technical results from the SIERRA sounding rocket experiment are comprehensive and are discussed in detail in [4] where the relationship between fields and particles is documented. Herein we summarize the results from the magnetic and electric field experiments.

4.1 Initial Electric and Magnetic Field Results

The initial electric field and magnetic field results from the SIERRA experiment are shown in Fig. 4. The three electric field measurements are shown in the top three

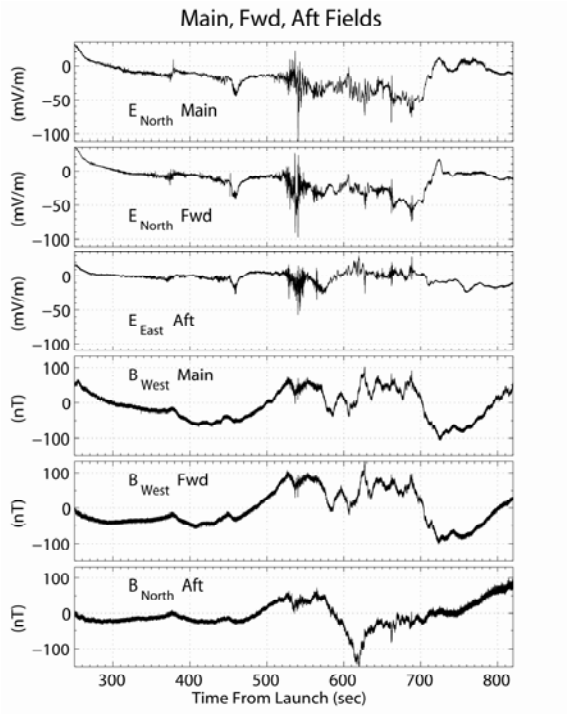

Figure 4. The initial electric field and magnetic field results for the SIERRA experiment.

panels. The electric field transverse to the geomagnetic field, assuming that the parallel electric field component is zero or near zero, is displayed. The lower three panels show the magnetic field along the

payload spin axes. This is preliminary data in that a full attitude solution has not been performed.

Fig. 4 illustrates several important points. First, the westward magnetic field perturbations as measured by the main and forward payloads were virtually identical. Since the magnetometers were on different payloads with different characteristics, this implies that the magnetic field perturbations are real. Before, when these perturbations were observed, there was no convincing way of demonstrating that we were measuring real magnetic fields. A comparison of the westward magnetic field perturbations on main and forward payloads makes a compelling argument for the accuracy and validity of the measurement.

The second feature seen in this data is increased levels of electric and magnetic field fluctuations seen in the data from 520 s to 700 s. The fluctuations have time scales from a few tens of seconds to less than one second; for example, at 520 s, rapid electric and magnetic fluctuations are apparent in both the electric and magnetic field records. The time-varying fields are evidence of an active auroral region with varying field-aligned currents and the fast fluctuations are evidence of Alfvén waves.

4.2 Final Electric and Magnetic Field Results

To obtain the final results, a precise attitude solution is required, which is described in [5]. The instruments for determining attitude are the magnetometer and a

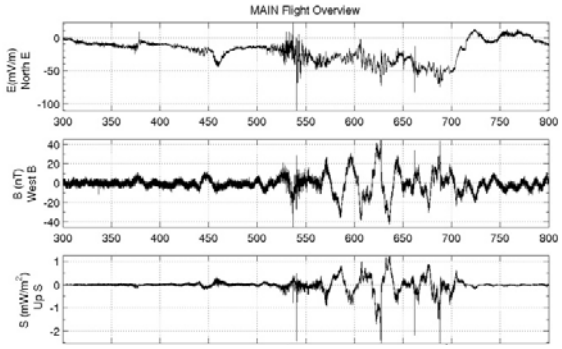

Figure 5. The calibrated electric field (top panel), westward magnetic field perturbations from IRGF (middle panel), and the Poynting vector (bottom panel).

horizon sensor. A form of Kalman filter is applied, creating an optimal attitude solution for the entire flight while conserving angular momentum and estimating errors in the magnetometer and horizon sensor measurements. This attitude solution is combined with the GPS positioning and the IGRF magnetic field to yield absolute magnetic field perturbations. Fig. 5 shows the absolute westward magnetic field perturbations in the middle panel, the northward electric field measurements in the top panel, and the Poynting vector over the flight in the bottom panel.

Now the Alfvén region is clearly visible in the Poynting vector record. Before 520 s, where there were relatively stable auroral arcs, the Poynting vector is small but from 520 s to 700 s, it becomes large and variable with equal amounts of upward and downward Poynting vector. The variable magnetic field perturbations are evidence of the payload passing through a region of both upward and downward field-aligned currents. Also, even in this compressed time

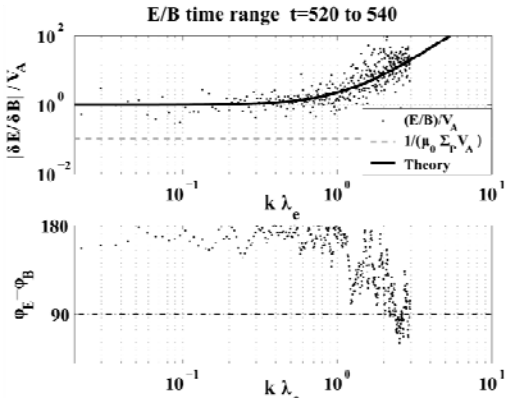

Figure 6. In the upper panel is the measured ratio of electric and magnetic field fluctuations as a function of perpendicular wave vector and in the lower panel is the relative phase of the electric and magnetic field fluctuations as a function of wave vector.

scale, fast variations are clearly visible around 540 s and these variations in both electric and magnetic field are Alfvén waves.

For an Alfvén wave in the limit of small $k_\perp$, the Alfvén velocity is independent of the wave perpendicular wave length and is given by

$$\delta E / \delta B = v_A = B / \sqrt{\mu_0 \rho} \qquad (1)$$

where B is the magnetic field, μ_0 is the permeability of free space, and ρ is the mass density. However, for finite $k_\perp$, this relation changes to

$$\delta E / \delta B = v_A \sqrt{1 + k_\perp^2 \lambda_e^2} \qquad (2)$$

where

$$\lambda_e = c / \omega_{pe} \qquad (3)$$

is the electron skin depth and for wavelengths long compared to the electron gyroradius. In the ionosphere, the electron skin depth is about 100 meters depending on the density and, when the second term in the square root becomes significant, the wave is called an inertial Alfvén wave.

Reference [4] tested the inertial Alfvén wave hypothesis by assuming that the small-scale electric and magnetic field fluctuations in the payload reference were spatial variations in the ionospheric frame. Knowing the payload perpendicular velocity, the ratio of $\delta E/\delta B$ to v_A can be calculated as a function of perpendicular wave vector ($k_\perp$). This result is shown in Fig. 6. In the upper panel is the measured ratio of $\delta E/\delta B$ to v_A as a function of the perpendicular wave vector. The estimated ratio for a static structure, not waves, is shown as the dashed line, so they are clearly not static structures. The solid line is the estimated ratio for an inertial Alfvén wave and the agreement is excellent. This also agrees with results from satellite measurements [6]. The phase shift as a function of perpendicular wave number in the lower plot suggests that the inertial Alfvén wave explanation is not complete and that, at small perpendicular wavelengths, the fluctuations are no longer propagating.

5. CONCLUSIONS

The poleward boundary of the active auroral oval is a region of rapidly varying Poynting flux, varying field-aligned current, and inertial Alfvén waves. These Alfvén waves are responsible for the hundreds of eV to keV field-aligned electrons that produce rayed auroral arcs and the rapid movement in rayed auroral arcs. At short perpendicular wavelengths, the inertial Alfvén waves likely are responsible for the transverse acceleration of heavy ions (O^+), which is the mass source for the ionosphere. Furthermore, sounding rocket payloads are an excellent platform for investigating these phenomena.

6. ACKNOWLEDGEMENTS

The author thanks his collaborators, Eric Klatt, Kristina Lynch, Charles Seyler, and Mark Psiaki. The design of the COWBOYS instrument was largely conducted by Steven Powell. This work was supported by National Aeronautics and Space Administration grants NAG5-5233, NAG5-12894, NAG5-12991, and grant NNX07AN38G.

7. REFERENCES

[1] Boehm, M.H., C.W. Carlson, J.P. McFadden, J.H. Clemmons, and F.S. Mozer, High-resolution sounding rocket observations of large amplitude Alfvén waves, *J. Geophys. Res.*, *95*(A8), 12,157-12,171, 1990.

[2] Lynch, K.A., J.W. Bonnell, C.W. Carlson, and W.J. Peria, Return current region aurora: $\mathbf{E}_\parallel$, $\mathbf{j}_z$, particle energization, and broadband ELF wave activity, *J. Geophys. Res.*, *107*(A7), 1115, doi:10.1029/2001JA900134, 2002.

[3] Powell, S.P., and P.M. Kintner, Using GPS for telemetry system clock generation and synchronization on-board sounding rockets, *Proceedings of ION GPS-96, The 9th International Technical Meeting of The Satellite Division of The Institute of Navigation*, published by The Institute of Navigation, Alexandria, Virginia, part 2, 1341-1348, 1996.

[4] Klatt, E.M., P.M. Kintner, C.E. Seyler, K. Liu, E.A. MacDonald, and K.A. Lynch, SIERRA observations of Alfvénic processes in the topside auroral ionosphere, *J. Geophys. Res.*, *110*, A10S12, doi:10.1029/2004JA010883, 2005.

[5] Humphreys, T.E., M.L. Psiaki, E.M. Klatt, S.P. Powell, and P.M. Kintner, Jr., Magnetometer-based attitude and rate estimation for spacecraft with wire booms, *J. Guid. Cont. Dyn.*, *28*(4), 584-593, 2005.

[6] Stasiewicz, K., et al., Small scale Alfvénic structure in the aurora, *Space Sci. Rev.*, *92*(3-4), 423–533, 2002.